RESEARCH PAPER

Early toll-like receptor 4 blockade reduces ROS and inflammation triggered by microglial pro-inflammatory phenotype in rodent and human brain ischaemia models

Esther Parada[1,2] | Ana I. Casas[3] | Alejandra Palomino-Antolin[1,2] |
Vanessa Gómez-Rangel[1,2] | Alfonso Rubio-Navarro[4] | Victor Farré-Alins[1,2] |
Paloma Narros-Fernandez[1,2] | Melania Guerrero-Hue[4] | Juan Antonio Moreno[4] |
Juliana M. Rosa[1,2] | José M. Roda[5] | Borja J. Hernández-García[5] | Javier Egea[1,2] (ID)

[1] Molecular Neuroinflammation and Neuronal Plasticity Research Laboratory, Hospital Universitario Santa Cristina, Instituto de Investigación Sanitaria-Hospital Universitario de la Princesa, Madrid, Spain

[2] Instituto Teófilo Hernando, Departamento de Farmacología y Terapéutica, Facultad de Medicina, UAM, Madrid, Spain

[3] Department of Pharmacology and Personalised Medicine, CARIM, Maastricht University, Maastricht, The Netherlands

[4] Renal, Vascular and Diabetes Research Lab, Instituto de Investigación Sanitaria-Fundación Jiménez Díaz, Universidad Autónoma de Madrid, Madrid, Spain

[5] Servicio de Neurocirugía, Hospital Universitario La Paz, Madrid, Spain

Correspondence
Javier Egea, Molecular Neuroinflammation and Neuronal Plasticity Research Laboratory, Hospital Universitario Santa Cristina, Instituto de Investigación Sanitaria-Hospital Universitario de la Princesa, Madrid, Spain.
Email: javier.egea@inv.uam.es

Funding information
Instituto de Salud Carlos III, Grant/Award Numbers: CP10/00479, CP14/00008, CPII16/00017, PI13/00802, PI14/00883 and PI16/00735; Fundacion Conchita Rábano; Spanish Ministry of Economy and Competitiveness, Grant/Award Number: RYC-2017-22369; Spanish Society of Nephrology and Fundación Renal Iñigo Alvarez de Toledo (FRIAT); Roche; Kootstra Talented Fellowship; Fundación Mutua Madrileña; Fondo de Investigaciones Sanitarias (FIS) (ISCIII/FEDER), Grant/Award Numbers: PI14/00883, PI13/00802, CPII16/00017, CP10/00479, PI16/00735 and CP14/00008

Background and Purpose: Ischaemic stroke is a leading cause of death, disability, and a high unmet medical need. Post-reperfusion inflammation and an up-regulation of toll-like receptor 4 (TLR4), an upstream sensor of innate immunity, are associated with poor outcome in stroke patients. Here, we identified the therapeutic effect of targeting the LPS/TLR4 signal transduction pathway.

Experimental Approach: We tested the effect of the TLR4 inhibitor, eritoran (E5564) in different in vitro ischaemia-related models: human organotypic cortex culture, rat organotypic hippocampal cultures, and primary mixed glia cultures. We explored the therapeutic window of E5564 in the transient middle cerebral artery occlusion model of cerebral ischaemia in mice.

Key Results: In vivo, administration of E5564 1 and 4 hr post-ischaemia reduced the expression of different pro-inflammatory chemokines and cytokines, infarct volume, blood–brain barrier breakdown, and improved neuromotor function, an important clinically relevant outcome. In the human organotypic cortex culture, E5564 reduced the activation of microglia and ROS production evoked by LPS.

Conclusion and Implications: TLR4 signalling has a causal role in the inflammation associated with a poor post-stroke outcome. Importantly, its inhibition by eritoran (E5564) provides neuroprotection both in vitro and in vivo, including in human tissue, suggesting a promising new therapeutic approach for ischaemic stroke.

Esther Parada and Ana I. Casas contributed equally to the work.

1 | INTRODUCTION

Inflammation takes place in both chronic and acute brain diseases and plays a key role in the development of several pathologies. Indeed, immune activation in the CNS is a common feature of brain injuries such as stroke, neurodegenerative diseases, and multiple sclerosis. Chronic inflammation leads to noxious effects on neurons and, thus, contributes to the pathophysiology of neurodegenerative diseases. Brain ischaemia is an acute injury that leads to the production of ROS and reactive nitrogen species (RNS), lipid peroxidation, blood–brain barrier (BBB) disruption, and exacerbated inflammation resulting in dramatic neuronal death (Chen et al., 2011). All together, these mechanisms contribute to severe tissue damage, defective regeneration, wound healing, and tissue repair aggravating patient outcome and a worsening prognosis after brain ischaemia (Aertker, Bedi, & Cox, 2016).

Microglia morphology and function are closely related. Microglial cells have been classified into three distinct subtypes according to shape: compact, longitudinally branched, and radially branched (Lawson, Perry, Dri, & Gordon, 1990). These morphologies are closely related to their functional state (Davis, Foster, & Thomas, 1994). Morphologically, the "resting" phenotype is characterized by a ramified morphology, which predominates under healthy conditions where microglia are continuously scanning their environment (Nimmerjahn, Kirchhoff, & Helmchen, 2005). Upon injury, ramified microglia turn into an "activated state," characterized by swollen ramified cells (larger cell body and shorter, thick processes), or an "alternatively reactive state" (small spherical cells or amoeboid-like morphology; Davis et al., 1994). Post-injury microglial cells are polarized to the pro-inflammatory phenotype (M1) producing cytokines, that is, TNF-α and IL-1β, or to an alternative anti-inflammatory phenotype (M2) where microglial cells express IL-10 and TGF-β. However, a dual role of microglia in cerebral ischaemia has been recently described. The microglia population has been shown to move from a M2 phenotype (first days after stroke) towards an M1 phenotype (several days after stroke; Hu et al., 2012), indicating that the M2-to-M1 shift during chronic inflammation post-stroke increases neuronal injury leading to poor recovery, a common pathological mechanism in CNS injuries.

Toll-like receptors (TLRs) belong to a class of transmembrane pattern-recognition receptor family that play a crucial role in the regulation of immune and inflammatory responses (Janssens & Beyaert, 2003). The TLR4 subtype is associated with several acute CNS pathologies, such as traumatic brain injury, subarachnoid haemorrhagic, and brain ischaemia (Arslan, Keogh, McGuirk, & Parker, 2010; Wang, Ge, & Zhu, 2013). Indeed, macrophage/microglia is the most important cell type expressing TLR4 contributing to the progression of injury (Vaure & Liu, 2014). Under ischaemic-dependent neurotoxic conditions, a plethora endogenous agonists of TLR4, such as Hsp60, Hsp70, and high mobility group box 1 (HMGB1) are dramatically increased (Yang et al., 2010; Yu, Wang, & Chen, 2010) resulting in activation of microglia pro-inflammatory responses and neuronal cell death (Kawasaki & Kawai, 2014). Deletion of TLR4 has a neuroprotective effect post-

What is already known
- E5564, a TLR4 antagonist, is protective in rodents against lethal influenza infection.
- Blockade of TLR4 signalling is considered to be a promising approach against acute brain damage.

What this study adds
- E5564 has a good therapeutic window in the tMCAO model of cerebral ischaemia in mice.
- E5564 protects against BBB breakdown, reduces cytokine expression and infarct volume, and thereby improves neuromotor function.

What is the clinical significance
- Repurposing of E5564 may be considered as a promising new therapeutic approach for ischaemic stroke.

stroke, which has resulted in blockade of TLR4 signalling being considered as a promising therapeutic approach (Hyakkoku et al., 2010).

Eritoran (E5564) is a synthetic analogue of lipid A and a potent TLR4 antagonist (Mullarkey et al., 2003). E5564 was shown to have protective effects in rodents against lethal influenza infection (Shirey et al., 2013) and liver or renal ischaemia/reperfusion (Liu et al., 2010; McDonald et al., 2014). During the next step, the efficacy of E5564 against sepsis reached an early clinical stage (Lynn et al., 2003; Tidswell et al., 2010). Unfortunately, E5564 failed to reduce the 28-day mortality rate in patients with severe sepsis (Opal et al., 2013). Nevertheless, there are several hypotheses that could explain this failure, (a) the activation of inflammatory pathways is determined by TLR4-independent mechanisms once septic shock is underway, (b) the pharmacological study was carried out with other TLR4 agonists distinct from LPS, or (c) the use of different inflammatory markers in patients enrolled in the trial (Opal et al., 2013; Tse, 2013). Thus, drug repurposing aims to accelerate currently unproductive drug discovery methods by finding new uses for existing drugs. The major advantage of the drug repurposing approach is that the safety issues have already been investigated in clinical trials.

In this context, we studied the protective role of E5564 in microglia inflammatory processes in organotypic cortical cultures of human brain samples as well as against in vitro and in vivo LPS-induced oxidative stress and cerebral ischaemia. By studying the effects on glial cells subjected to oxidative stress and an inflammatory environment, we provide evidence that TLR4 blockage with E5564 reduces the expression of pro-inflammatory markers in microglia, prevents BBB disruption and infarct volume, and even more importantly improves neurological outcome in rodents. These findings indicate that TLR4 signalling is an important pathway for determining the outcome of brain injuries and its blockage by E5564 supports a neuroprotective effect of this compound against brain ischaemia.

2 | METHODS

2.1 | Study design

All animal experiments were performed after approval of the protocol by the Ethics Committee of Autonomous University of Madrid (Madrid, Spain) according to the European Guidelines for the use and care of animals for research. Animal studies are reported in compliance with the ARRIVE guidelines (Kilkenny, Browne, Cuthill, Emerson, & Altman, 2010) and with the recommendations made by the *British Journal of Pharmacology*. All efforts were made to minimize animal suffering and to reduce the number of animals used in the experiments. Animals were housed under controlled conditions (22 ± 1°C, 55–65% humidity, 12-hr light–dark cycle) and had free access to water and standard laboratory chow. We used female and male C57Bl6J (3–4 months, 20–25 g or 25–30 g, respectively) supplied by the animal facilities of Universidad Autónoma de Madrid (Madrid, Spain. IMSR Cat# JAX:000664, RRID:IMSR_JAX:000664). Mice were subjected to transient middle cerebral artery occlusion (tMCAO) and, after cerebral ischaemia, animals were randomly divided into the following experimental groups: saline and E5564 (50% female and 50% male in each group). At the end of the experiment, animals were killed by cervical dislocation. Animals were excluded from endpoint analyses if (a) death occurred within 24 hr post-surgery and (b) intracerebral haemorrhage was detected. No mice were considered to qualify as a dropout in the vehicle and treatment groups (1 and 4 hr PO, 2,3,5-triphenyltetrazolium chloride [TTC]), whereas one mouse was discounted in the Evans Blue group (Table 1). Post hoc power analysis for adult mice is included in Table 2.

2.2 | Microglia BV2 cell line

BV2 cells (murine microglia, RRID:CVCL_0182) were maintained in RPMI medium 1640 supplemented with 10% FBS and antibiotics (penicillin 100 U·ml^{-1}, streptomycin 100 μg·ml^{-1}). Cultures were seeded into flasks containing supplemented medium and kept at 37°C in a humidified atmosphere of 5% CO_2 and 95% air. For assays, BV2 cells were subcultured in 48-well plates at a seeding density of 1×10^5 cells

TABLE 1 Animals excluded from the statistical analysis after tMCAO

Animal	Ischaemia model	Experiment duration (hr)	Excluded animal
C57/Bl6J	tMCAO−1 hr PO (TCC)	24	0 of 5
C57/Bl6J	tMCAO−1 hr PO (TCC)	24	0 of 11
C57/Bl6J	tMCAO−4 hr PO (TCC)	24	0 of 6
C57/Bl6J	tMCAO−Evans Blue	24	1 of 5
C57/Bl6J	tMCAO−ROS/RNS	24	0 of 5

Note. Animal exclusion procedures are described in the respective sections of the Methods.

Abbreviations: tMCAO, transient occlusion of the middle cerebral artery; TTC, 2,3,5-triphenyltetrazolium hydrochloride.

TABLE 2 Study design: Power analysis

Adult mice—tMCAO–Eritoran (4 mg·kg^{-1})				
	Mean	SD	n	Power for measured difference (%)
Infarct size (mm^3)				
Vehicle	110.1	21.5	6	80.1
Treatment 1 hr p.o.	67.5	20.8	11	
Treatment 4 hr p.o.	70.1	16.4	6	76.8
Four limb hanging				
Vehicle	41.7	37.3	6	83.6
Treatment 1 hr p.o.	99.5	37.2	11	
Elevated body swing				
Vehicle	0.8	0.8	6	96.0
Treatment 1 hr p.o.	2.0	2.1	11	

Note. We conducted a post hoc analysis of power in the different animal groups. For each animal treatment group, a pooled variance of the vehicle and treatment groups was calculated from mean, SD, and with *n* the size of the group and CV the coefficient of variation (SD/Mean) of the group. Power was calculated for the measured difference using Russ Lenth's power software with an α of .05, the measured effect (%), and the calculated pooled variances (Lenth, R. V 2006-9, java Applets for Power and Sample Size [Computer Software], Retrieved 02-17-2014, from http://www.stat.uiowa.edu/~rlenth/Power).

Abbreviations: *n*, number of animals; tMCAO, transient middle cerebral artery occlusion.

per well. Cells were treated with LPS (Sigma-Aldrich, Madrid, Spain), HMGB1 (Sigma-Aldrich, Madrid, Spain), resatorvid (TAK242, Sigma-Aldrich, Madrid, Spain), and E5564 (Eisai Research Institute, Boston, USA) before confluence in RPMI with 1% FBS.

2.3 | Mixed glial cultures

Mixed glial cultures were prepared from cerebral cortices of 3-day-old mice as previously described (Parada et al., 2015). Briefly, after removal of the meninges and blood vessels, the forebrains were gently dissociated by repeated pipetting in DMEM/F12 medium. After mechanical dissociation, cells were seeded in DMEM/F12 with 20% FBS at a density of 300,000 cells ml^{-1} and cultured at 37°C in humidified 5% CO_2/95% air. Medium was replaced after 5 days in vitro (DIV) by DMEM/F12 and 10% FBS. Confluence was achieved after 10–12 DIV, and cultures were treated with LPS (Sigma-Aldrich) and E5564 (Eisai Research Institute) in DMEM/F12 with 1% FBS.

2.4 | Griess reaction

The NO assay was performed using the previously reported protocols. Briefly, 100 μl of culture supernatants was mixed with the same volume of Griess assay reagent (1% sulfanilamide [Sigma Aldrich, Madrid], 0.1% naphthylethylenediamine dihydrochloride, and 2.5% phosphoric acid). Ten minutes later, the absorbance was measured at 560-nm.

2.5 | ROS measurement

To measure cellular ROS, we used the molecular probe H_2DCFDA. Glial cells were loaded with 5-μM H_2DCFDA as described previously (Parada et al., 2015). Fluorescence was measured in a fluorescence microplate reader (FLUOstar Galaxy; BMG Labtech, Offenburg, Germany). Wavelengths of excitation and emission were 485 and 520 nm respectively. The relative pixel intensity was measured in identical regions with ImageJ software (National Institutes of Health, USA).

2.6 | Determination of cytokine levels in the culture medium

After the different drug treatments, TNF-α levels were measured by using a specific ELISA kit. Supernatant samples were obtained at the indicated times and subjected to the ELISA analysis according to the manufacturer's recommendations (Prepotech, Spain).

2.7 | Quantitative real-time PCR

Total RNA from glial cultures were obtained by TRIzol method (10296-028, Invitrogen, Carlsbad, CA, USA) and reverse transcribed with a High Capacity cDNA Archive Kit, and real-time PCR was performed on a ABI Prism 7500 PCR system (Applied Biosystems, Foster City, CA, USA) using the Δ-Δ Ct method. Expression levels are given as ratios to ribosomal 18 s subunit (18 s). Expression of target genes was analysed by real-time quantitative PCR using TaqMan® gene expression assays.

2.8 | Animals and preparation of rat OHCs

Rat organotypic hippocampal cultures (rOHCs) were obtained from 8- to 10-day-old Sprague–Dawley rats (RGD Cat# 70508, RRID: RGD_70508) supplied by the animal facilities of Universidad Autónoma de Madrid (Madrid, Spain). Cultures were prepared according to the methods described by Stoppini, Buchs, and Muller (1991) with some modifications (Parada et al., 2013). Briefly, 300-μm-thick hippocampal slices were prepared using a McIlwain tissue chopper and separated in ice-cold HBSS composed of (mM) glucose 15, $CaCl_2$ 1.3, KCl 5.36, NaCl 137.93, KH_2PO_4 0.44, Na_2HPO_4 0.34, $MgCl_2$ 0.49, $MgSO_4$ 0.44, $NaHCO_3$ 4.1, and HEPES 25; 100-U·ml^{-1} penicillin and 0.100-mg·ml^{-1} gentamicin. Approximately 4–6 slices were placed on a Millicell 0.4-μm culture insert (Millipore) within each well of a six-well culture tray with the medium, where they remained for 7 days. The culture medium, which consisted of 50% minimal essential medium, 25% HBSS, and 25% heat-inactivated horse serum, were purchased from Life Technologies. The medium was supplemented with 3.7-mg·ml^{-1} d-glucose, 2-mmol·l^{-1} l-glutamine, and 2% of B-27 Supplement Minus antioxidants (Life Technologies, Madrid), and 100-U·ml^{-1} penicillin. OHCs were cultivated in a humidified atmosphere at 37°C and 5% CO_2, and the medium was changed twice a week.

2.9 | Oxygen–glucose deprivation in rOHCs

Oxygen–glucose deprivation was used as an in vitro model of cerebral ischaemia. The inserts with slice cultures were placed in 1 ml of oxygen and glucose deprivation (OGD) solution composed of the following (in mM): NaCl 137.93, KCl 5.36, $CaCl_2$ 2, $MgSO_4$ 1.19, $NaHCO_3$ 26, KH_2PO_4 1.18, and 2-deoxyglucose 11 (Sigma-Aldrich, Madrid). The cultures were then placed in an airtight chamber (Billups and Rothenberg) and exposed for 5 min to 95% N_2/5% CO_2 gas flow to ensure oxygen deprivation. After that, the chamber was sealed for 15 min at 37°C. The control cultures were maintained for the same time under a normoxic atmosphere in a solution with the same composition as that described above (OGD solution), but containing glucose (11 mM) instead of 2-deoxyglucose. After the OGD period, the cultures were returned to their original culture conditions for 24 hr (reoxygenation period).

2.10 | Quantification of cell death in rOHCs: Propidium iodide uptake

Cell death was determined in the CA1 region by staining the OHCs with propidium iodide (PI); 30 min before analysing fluorescence, slices were incubated with PI (1 μg·ml^{-1}) and Hoechst (1 μg·ml^{-1}); Hoechst staining was used to normalize PI fluorescence with respect to the number of nuclei. Fluorescence was measured in a fluorescence-inverted NIKON Eclipse T2000-U microscope. The wavelengths of excitation and emission for PI and Hoechst were 530 or 350, and 580 or 460 nm respectively. Images were taken at CA1 at magnifications of 10×. The Metamorph programme version 7.0 was used for fluorescence analysis (RRID:SCR_002368). To calculate cell death, we divided the mean PI fluorescence by the mean Hoechst fluorescence.

2.11 | Preparation of human organotypic cortical cultures

Cultures were prepared according to the methods described by Stoppini et al. (1991) with some modifications. Neurosurgical staff obtained written witnessed informed consent from patients undergoing a brain lobectomy. The consent for research purposes was obtained before surgery in all cases. Small brain tissue samples were obtained from pathology specimens. Briefly, 300-μm-thick cortical slices were prepared from human cortical tissue using a McIlwain tissue chopper and separated in ice-cold HBSS composed of (mM) glucose 15, $CaCl_2$ 1.3, KCl 5.36, NaCl 137.93, KH_2PO_4 0.44, Na_2HPO_4 0.34, $MgCl_2$ 0.49, $MgSO_4$ 0.44, $NaHCO_3$ 4.1, and HEPES 25; 100-U·ml^{-1} penicillin and 0.100-mg·ml^{-1} gentamicin. Approximately 2–3 slices were placed on Millicell 0.4-μm culture insert (Millipore) within each well of a six-well culture tray with the medium, where they remained for 7 days. The culture medium consisted of 50% minimal essential medium, 25% HBSS, and 25% heat-inactivated horse serum. The medium was supplemented with 3.7-mg·ml^{-1} d-glucose,

2-mmol·l^{-1} l-glutamine, 2% of B-27 Supplement Minus antioxidants (Life Technologies), and 100-U·ml^{-1} penicillin. Human organotypic cortical cultures (hOCCs) were cultivated in a humidified atmosphere at 37°C and 5% CO_2, and the medium was changed twice a week. After 7 DIV, hOCCs were treated with LPS 10 μM with or without E5564.

2.12 | In vivo transient MCAO ischaemia model

This mouse model was established as described by Kleinschnitz et al. (2010). C57Bl6/J mice were anaesthetized with isoflurane (0.8% in oxygen), placed on a heating pad, and rectal temperature was maintained at 37.0°C using a servo-controlled rectal probe-heating pad (Cibertec, Spain). Transient cerebral ischaemia was induced using the intraluminal filament technique. Using a surgical microscope (Tecnoscopio OPMI pico, Carl Zeiss, Meditec Iberia SA, Spain), a midline neck incision was made and the right common and external carotid arteries were isolated and permanently ligated. A microvascular temporarily ligature was placed on the internal carotid artery to cut non-permanently the blood flow. A silicon rubber-coated monofilament (6023910PK10, Doccol Corporation, Sharon, MA, USA) was inserted through a small incision into the common carotid artery and advanced into the internal carotid artery until a resistance was felt. The tip of the monofilament should be precisely located at the origin of the right middle cerebral artery and thus interrupting blood flow. The filament was held in place by a tourniquet suture in the common carotid artery to prevent filament relocation during the ischaemia period. Animals were maintained under anaesthesia during the 1-hr occlusion period followed by the reperfusion period which started when the monofilament was removed. After the surgery, wounds were carefully sutured and animals were allowed to recover from surgery in a temperature-controlled cupboard. Animals were provided with post-operative analgesia (0.5% lidocaine, s.c.). Operation time per animal did not exceed 15 min. Animals were excluded from the stroke analysis, if they died within the first 24 hr, if an intracerebral haemorrhage occurred, or in cases where the animal scored 0 on the Bederson scale.

2.13 | Determination of infarct volume

After the mice had been killed, brains were quickly removed and cut in four 2-mm-thick coronal sections using a mouse brain slice matrix (Harvard Apparatus, Spain). The slices were stained for 15 min at room temperature with 2% TTC (Sigma-Aldrich, the Netherlands) in PBS to visualize the infarctions (Bederson, Pitts, Germano, et al., 1986). Indirect infarct volumes were calculated by volumetry (ImageJ software, National Institutes of Health) according to the following equation: $V_{indirect}$ (mm^3) = $V_{infarct}$ × (1 − (V_{ih} − V_{ch})/V_{ch}), where the term (V_{ih} − V_{ch}) represents the volume difference between the ischaemic hemisphere and the control hemisphere and (V_{ih} − V_{ch})/V_{ch} expresses this difference as a percentage of the control hemisphere.

2.14 | Assessment of neuromotor functional outcomes

Three different neuromotor functioning tests were assessed in all mice groups (male, female, and middle aged) treated 1 or 4 hr after filament removal. The Bederson scale (Bederson, Pitts, Tsuji, et al., 1986) is defined by: Score 0, no apparent neurological deficits; 1, body torsion and forelimb flexion; 2, right side weakness and thus decreased resistance to lateral push; 3, unidirectional circling behaviour; 4, longitudinal spinning; and 5, no movement. Within the elevated body swing test, a mouse was held ~1 cm from the base of its tail and then elevated above the surface in the vertical axis around 20 cm. We considered a swing whenever the animal moved its head out of the vertical axis to either the left or the right side (more than 10°). Ratio of right/left swings were subsequently analysed. Finally, to directly evaluate strength, the four-limbs hanging wire test was performed. The mouse was placed on the centre of the wire with a diameter of 10 cm. Later, the wire was slowly inverted and placed at ~40 cm above paper towel bedding. The time until the mouse fell from the wire was recorded, with a maximum time of 120 s.

2.15 | Determination of BBB leakage and brain oedema

To determine the permeability of the cerebral vasculature and brain oedema formation after 1-hr occlusion of the tMCAO, 2% Evans Blue tracer (Sigma Aldrich, the Netherlands) was diluted in 0.9% NaCl and then injected i.p. just after removal of the filament. Measurement of Evans Blue extravasation was performed as described by Kleinschnitz et al. (2010).

2.16 | Oxidative stress: DHE staining

ROS production by in vivo brain tissue was determined using the florescence dye dihydroethidium (Thermo Scientific Technology, the Netherlands) obtained from a 2-mM stock solution. Frozen brain cryosections were fixated in 4% paraformaldehyde in PBS and then incubated with 2-μM DHE for 30 min at 37°C. After three washing steps with PBS, slices were incubated with Hoechst (Hoechst 33342, Sigma-Aldrich, the Netherlands) 2 ng·ml^{-1} for 10 min at 37°C. The relative pixel intensity was measured in identical regions with ImageJ software (National Institutes of Health).

2.17 | Immunohistochemistry: N-Tyr staining

Brain tissue cryosections (10 μm) were fixed with 4% PFA in PBS. After a 1-hr blockade, sections were incubated for 1 hr at room temperature with a rabbit polyclonal anti-nitrotyrosine antibody (1:100; Thermo Fisher Scientific, Cat# A-21285, RRID:AB_221457) in blocking buffer. After three washes in PBS, sections were incubated with the secondary antibody, Alexa Fluor 488 donkey anti-rabbit

(1:100; Thermo Fisher Scientific, Cat# A-21206, RRID:AB_2535792), for 45 min at room temperature. Then, the fluorescent Hoechst 33342 dye (2 ng·ml^{-1}; Thermo Fisher Scientific, the Netherlands) was added for 10 min at room temperature. Sections were washed in PBS and then mounted using a Dako Fluorescence Mounting Medium (S3023, Agilent Technologies). Immunofluorescent signals were viewed using a Leica DMI3000 B fluorescence microscope. Quantitative analysis of nitrotyrosine fluorescence was performed with ImageJ software (National Institute of Health; RRID: SCR_003070).

2.18 | Immunoblotting and image analysis

After the different treatments, glial cells were washed once with cold PBS and lysed in 100-μl ice-cold lysis buffer (1% Nonidet P-40, 10% glycerol, 137-mM NaCl, 20-mM Tris–HCl, pH 7.5, 1-g·ml^{-1} leupeptin, 1-mM PMSF, 20-mM NaF, 1-mM sodium pyrophosphate, and 1-mM Na$_3$VO$_4$). Proteins (30 μg) from the cell lysate were resolved by SDS–PAGE and transferred to Immobilon-P membranes (Millipore Corp., Billerica, MA, USA). Membranes were incubated with anti-p-IκB-α (1:500; Santa Cruz Biotechnology, Santa Cruz, CA, USA), anti-iNOS (1:1,000; Santa Cruz Biotechnology, Santa Cruz, CA, USA), anti-β actin (1:100,000; Sigma), anti-Iba1 (1:1,000; ionized calcium-binding adapter molecule 1; Wako Chemicals, Rafer S. L, Madrid, Spain. Cat# 019-19741, RRID:AB_839504). Appropriate peroxidase-conjugated secondary antibodies (1:10,000) were used to detect proteins by enhanced chemiluminescence. Different band intensities corresponding to immunoblot detection of protein samples were quantified using the Scion Image program (RRID:SCR_008673). Immunoblots correspond to a representative experiment that was repeated three or four times with similar results.

2.19 | Immunofluorescence and immunohistochemistry

The protocol was as previously described by Parada et al. (2013). After the different drug treatments, OHC slices were fixed with 2% paraformaldehyde dissolved in PBS for 15 min and washed three times with PBS every 5 min. Later, OHCs were labelled with rabbit anti-Iba1 (1:100, Wako Chemicals) and the nuclei stained with Hoechst (5 μg·ml^{-1}). For immunohistochemistry assays, the endogenous peroxidase was inactivated with 1% H$_2$O$_2$, and the slices were then incubated in a blocking solution (PBS, 10% BSA, and 10% normal goat serum) for 1 hr, and rabbit anti-Iba1 was used as the primary antibody 1:1,000 (Wako Chemicals, Rafer S.L.) overnight. The secondary antibody was biotinylated goat anti-rabbit (Vector Labs; 1:200; 2 hr) and was dissolved in a blocking solution. The slices were incubated in an avidin–biotin peroxidase complex (Kit ABC Elite®, 1:250 in PBS; Vector Laboratories) for 2 hr and reacted with diaminobenzidine (0.05%; Sigma) with H$_2$O$_2$ (0.003% of the stock 30% solution). The intensity of the staining was checked every few minutes under a microscope, and when labelling was satisfactory, the reaction was stopped by

rinsing the slices with a cold PB. After several washes with PB, the slices were dehydrated in ethanol, defatted with xylene, and coverslipped with DePeX. Negative controls for the specificity of the secondary antibody were prepared by omitting the primary antibody. For microglia morphology quantification, two observers blind to the samples identity quantified the number of Iba1 positive cells in each image of the slice (rat or human; Leica microscope at a 40× magnification). Images were analysed by two blinded observers. Positive-stained cells were counted in five different fields per experiment, in six independent experiments. We used the media of the two blinded observers for each image and quantified five images per variable. The immuno-related procedures used comply with the recommendations made by the British Journal of Pharmacology.

2.20 | Data and statistical analysis

The data and statistical analysis comply with the recommendations of the British Journal of Pharmacology on experimental design and analysis in pharmacology (Curtis et al., 2018). Mice were randomly assigned to each treatment group and experiment. Also data analysis was performed in a manner completely blind to experimental groups. Firstly, data were tested with a Shapiro–Wilk test for normality and Levene's test for equality of variance. Sex differences in infarct size, brain oedema, and neuromotor functional tests were analysed by a two-way ANOVA. Since no sex difference was observed in any of these experiments, data from both male and female mice were pulled and analysed together. All results are expressed as mean ± SEM except for ordinal functional outcome scales that were depicted as scatter plots. Student's two-tailed unpaired t test (Gaussian distribution) or Mann–Whitney U-test (non-Gaussian distribution) was used to analyse significant differences between two groups. Ordinary one-way ANOVA with Newman–Keuls multiple comparison posttest (Gaussian distribution) was used to compare variables among three or more groups. The number of animals necessary to detect a standardized effect size on infarct volumes ≥0.2 (vehicle treated control mice vs. treated mice) was determined via a priori sample size calculation with the following assumptions: α = .05, β = .2, mean, 20% SD of the mean. The threshold for statistical significance was $P < .05$ throughout. All results were analysed using the GraphPad Prism 6.0 software (GraphPad Software Inc., San Diego, CA, USA. RRID:SCR_002798). All measurements were undertaken in at least three technical replicates.

2.21 | Nomenclature of targets and ligands

Key protein targets and ligands in this article are hyperlinked to corresponding entries in http://www.guidetopharmacology.org, the common portal for data from the IUPHAR/BPS Guide to PHARMACOLOGY (Harding et al., 2018), and are permanently archived in the Concise Guide to PHARMACOLOGY 2015/16 (Alexander, Fabbro et al., 2017a,b; Alexander, Kelly et al., 2017).

3 | RESULTS

3.1 | E5564 blocks TLR4 and reduces oxidative stress induced by LPS treatment in BV2

In the canonical NF-κB pathway, TLR4 agonists activate IκB kinase (IKK), which results in the phosphorylation of IκB-α causing its ubiquitination and degradation. This process enables p65 and p50 subunits of NF-κB to translocate to the nucleus, which results in the production of ROS due to the production of inducible NOS (iNOS) and COX-2 and the secretion of inflammatory cytokines/chemokines. Hence, we examined whether E5564 and TAK242 regulate LPS-stimulated IκB-α phosphorylation in BV2 microglia cells. We used microglial BV2 cells incubated with 1-μg·ml^{-1} LPS or 0.2-μg·ml^{-1} HMGB1 for 30 min, in the absence or presence of E5564 (1 μM) or

TAK242 (1 μM). LPS and HMGB1 significantly increased IκB-α phosphorylation and this was prevented by TAK242 and by E5564 (Figure 1a–b). Next, we assessed ROS/RNS production using different approaches: (a) nitrite production, (b) iNOS, and (c) ROS production. Microglial BV2 cells were incubated with 1-μg·ml^{-1} LPS or 0.2-μg·ml^{-1} HMGB1, in the absence or the presence of E5564 (0.1 or 1 μM) or TAK242 (1 μM) during 24 hr. LPS and HMGB1 significantly increased nitrite production and this was prevented by TAK242 and by E5564 cotreatment in a concentration-dependent manner (Figure 1c–d). Moreover, iNOS expression induced by LPS and HMGB1 was down-regulated by both compounds (Figure 2a–b). In addition, treatment with LPS for 24 hr tripled the amount of ROS produced in BV2 microglia cells compared to basal and E5564 at 1 μM reduced LPS-mediated ROS production almost to control levels (Figures 2c–i).
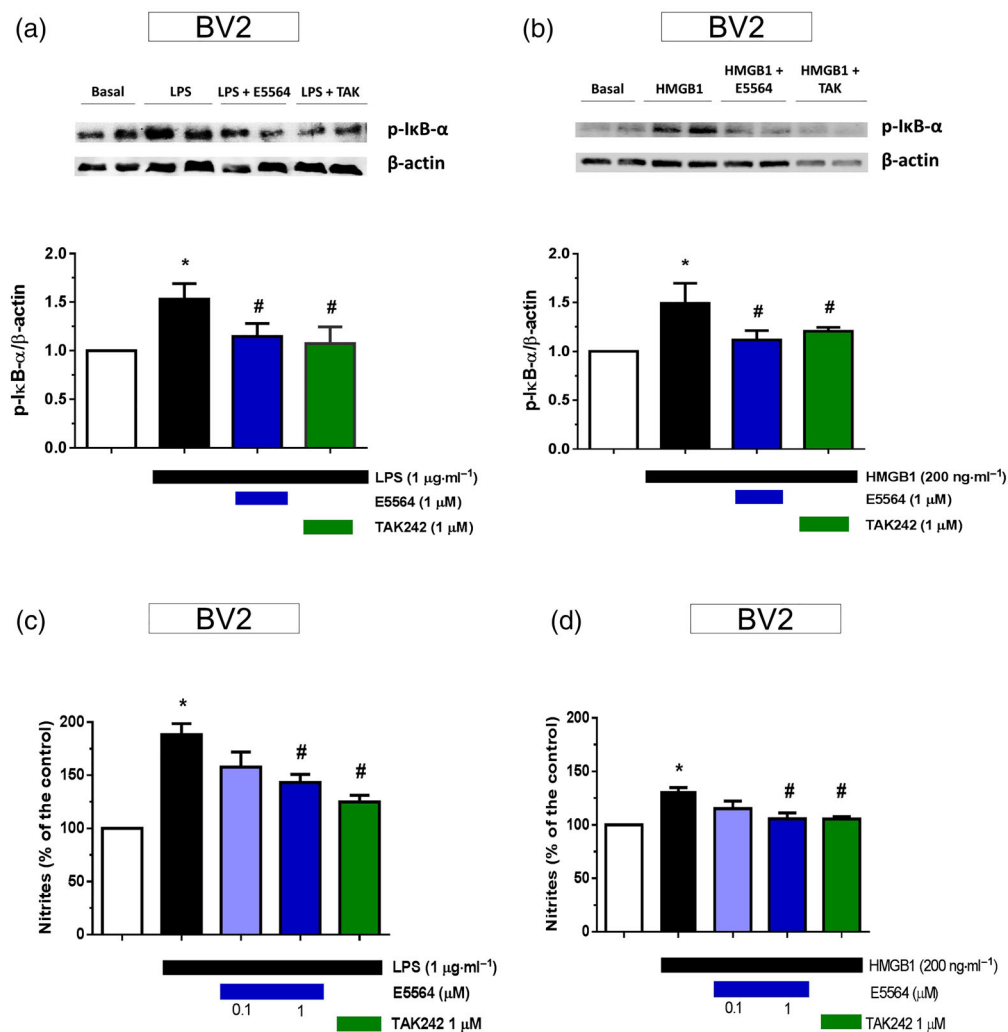
FIGURE 1 E5564 blocks TLR4 and reduces ROS production in BV2 cells. Representative immunoblot of IκB-α from cells treated with LPS 1 μg·ml^{-1} (a) or HMGB1 200 ng·ml^{-1} (b) with or without E5564 (1 μM) or TAK242 (1 μM) for 30 min. Both compounds reduced IκB-α phosphorylation in the presence of TLR4 agonists. Cells were treated with LPS 1 μg·ml^{-1} (c) or HMGB1 200 ng·ml^{-1} (d) with or without E5564 (0.1 and 1 μM) or TAK242 (1 μM) for 24 hr. Both concentrations of E5564 and TAK242 reduced the production of nitrites in the presence of TLR4 agonists. Values are expressed as means ± SEM of five different cell batches; *$P < .05$ compared to basal; #$P < .05$ in comparison with LPS/ HMGB1-treated cells
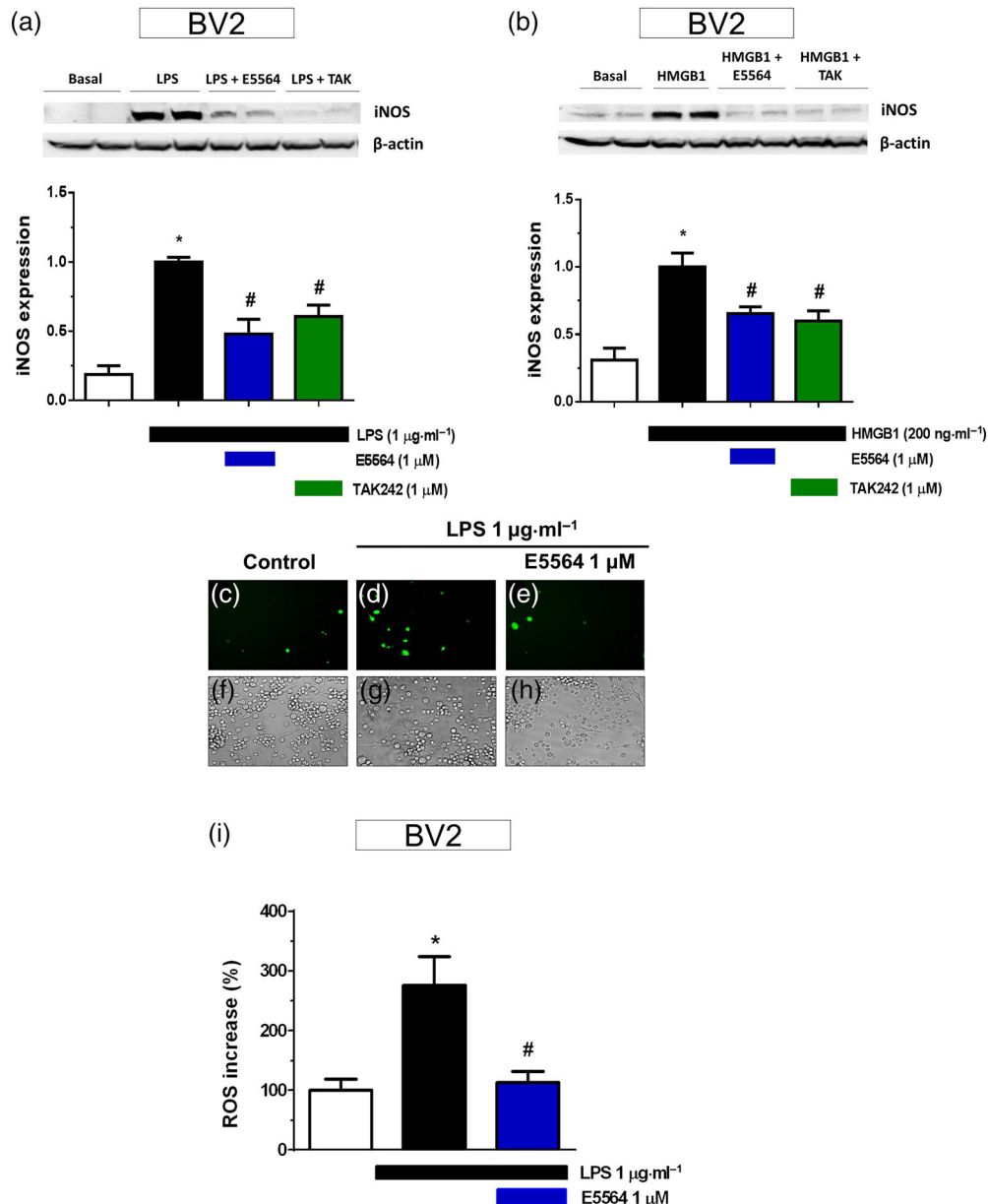
FIGURE 2 Anti-inflammatory and antioxidant effect of E5564 in BV2 microglial cells. Representative immunoblot of iNOS from untreated cells (Track 1–2), cells incubated for 24 hr with LPS (Track 3–4), and cells co-incubated for 24 hr with LPS in the presence of 1-μM E5564 or TAK242 (Track 5–6 and 7–8 respectively). (c–h) Photomicrographs (original magnification 20×) of cells loaded with the fluorescent probe H$_2$DCFDA are shown. (c) Untreated cells, (d) cells incubated for 24 hr with LPS, and (e) cells incubated with LPS plus 1-μM E5564. (f–h) Photomicrographs of non-loaded cells under the same experimental procedures. (i) Effect of E5564 on ROS production elicited by LPS treatment. Values are expressed as means ± SEM of five different cell batches; *$P < .05$ compared to basal; #$P < .05$ in comparison with LPS/HMGB1-treated cells

3.2 | Antioxidant and anti-inflammatory effects of E5564 in primary glial cultures

To confirm the results obtained in BV2 microglia cells, we measured nitrite release and ROS production in mixed glial primary cultures treated with LPS for 24 hr and co-incubated with E5564. Under this experimental protocol, E5564 reduced nitrite release (Figure 3a) and ROS production (Figure 3b) induced by LPS. It is well known that TLR4 activation initiates the systemic inflammatory response mediated by the innate immune system producing an acute increase in several pro-inflammatory cytokines and chemokines (Kawasaki &

Kawai, 2014). Hence, we evaluated mRNA levels of two chemokines (CCL2 and CCL5) as well as pro-inflammatory cytokines (TNF-α, IL-1β, and IL-6). For this purpose, mixed glia cultures were treated with LPS in the presence or absence of E5564 for 2 hr and mRNA expression was measured by quantitative PCR. E5564 prevented LPS-mediated mRNA increase of all chemokines and cytokines studied (Figure 3c). To further corroborate the anti-inflammatory properties of E5564, TNF-α concentration was quantified by ELISA in the culture medium of mixed glia cells (Figure 3d). Treatment of mixed glia cultures with E5564 significantly reduced LPS-mediated TNF-α concentration. These findings suggest that E5564 inhibits the
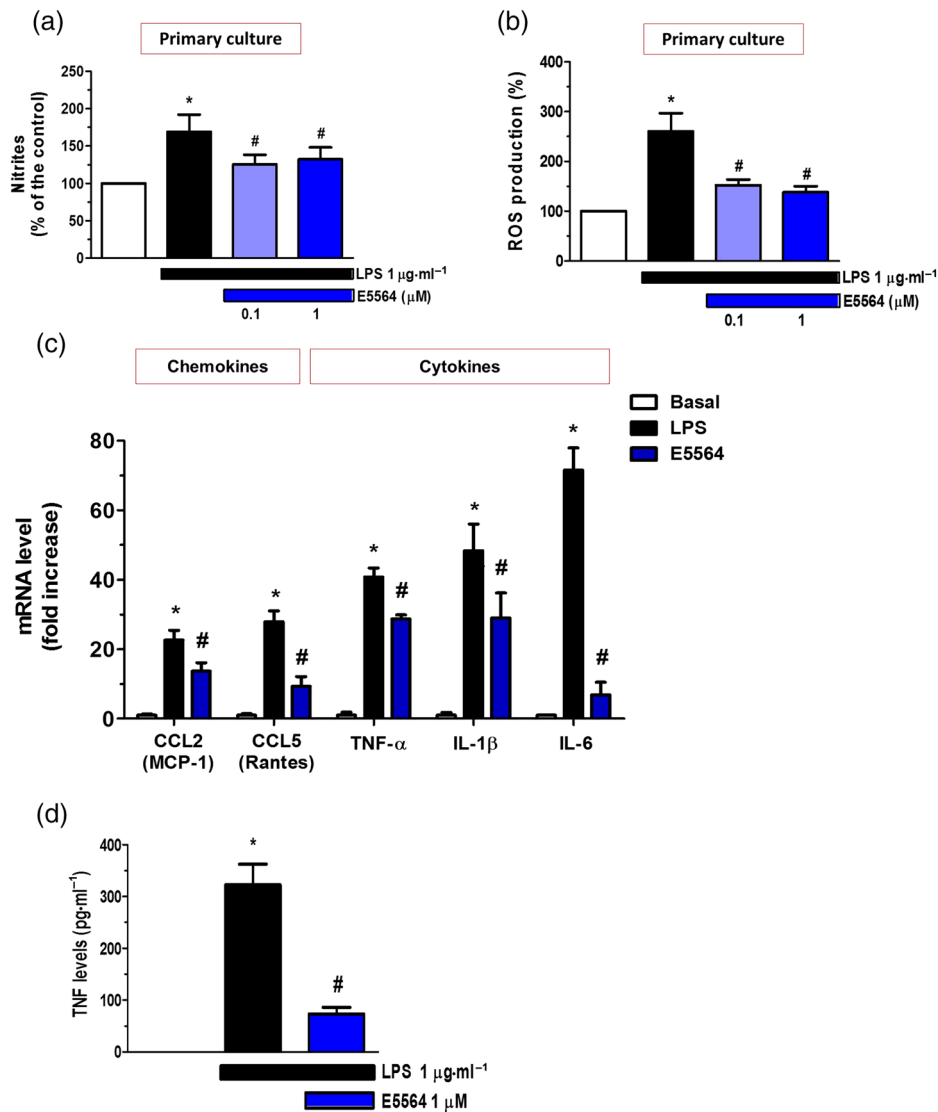
**FIGURE 3** Anti-inflammatory effect of E5564 in primary cultures of mixed microglia. Mixed glia cultures were treated with LPS 1 μg·ml⁻¹ with or without E5564 at 0.1 and 1 μM for 24 hr. Cells treated with E5564 had reduced (a) nitrite and (b) ROS production in response to LPS. (c) Cytokines (TNF-α, IL-1β, and IL-6) and chemokines (CCL2 and CCL5) mRNA levels of mixed glia cultures treated with LPS 1 μg·ml⁻¹ in the presence or absence of 1-μM E5564 for 2 hr. (d) Release of TNF-α in mixed glia culture supernatant treated with 1-μM-E5564 for 24 hr. Values are expressed as means ± SEM of at least five different cell cultures; *$P < .05$ compared to basal; #$P < .05$ in comparison with LPS-treated cells

production of pro-inflammatory cytokines and chemokines in primary glia cultures.

3.3 | Neuroprotective and anti-inflammatory effect of the TLR4 antagonist E5564 in rat OHCs post-OGD administration

Once we had defined the anti-inflammatory action of E5564 against LPS-induced inflammation in BV2 and primary microglia, we evaluated the anti-inflammatory action of E5564 in OHCs. Following the protocol shown in Figure 4a, OHCs were subjected to 15 min of OGD followed by 24 hr of reoxygenation where E5564 was present. After reoxygenation, cell death was assessed by PI fluorescence in the hippocampal area CA1. Under these experimental conditions, increasing

concentrations of E5564 (0.1 and 1 μM) reduced cell death post-OGD treatment to basal levels (Figure 4a). To further evaluate the changes in microglial phenotype post-OGD, OHCs were fixed with paraformaldehyde 4% and immunofluorescence of Iba1 (specific microglial marker) was performed under each experimental condition (Figure 4b), and morphological phenotype of microglia were quantified and classified according to the different states of activation as described in Figure 4c: Type 1, resting microglia; Type 2, initiation of microglial activation; Type 3, activated but non-phagocytic; and Type 4, activated phagocytic (Sanchez-Guajardo, Febbraro, Kirik, & Romero-Ramos, 2010). In these conditions, OHCs subjected to OGD had significantly less Type 1 microglial cells. We also observed an increase in microglia Type 3 and Type 4 microglial cells. Interestingly, OHCs treated with E5564 exhibited significantly fewerType 3 and Type 4 microglia cells (Figure 4d). Moreover, by measuring the cell body
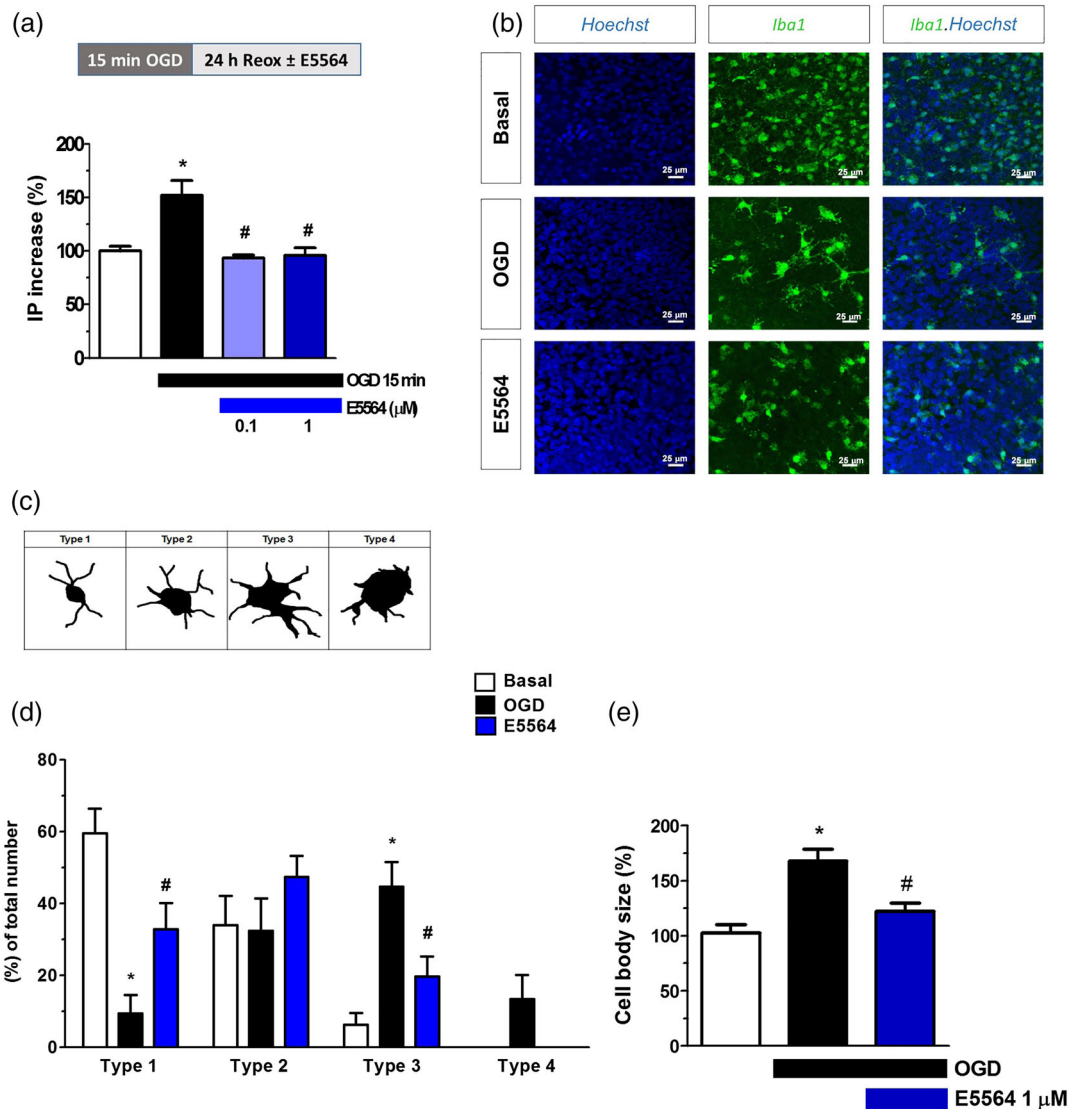
FIGURE 4 E5564 had a protective effect in OHCs and reduced microglia activation. (a) OHCs were exposed for 15 min to OGD followed by 24 hr of reoxygenation (Reox) in the presence or absence of E5564 (0.1 and 1 μM) for 24 hr. Cell death was measured by IP florescence in CA1. (b) Immunofluorescence of OHCs labelled with anti-Iba1 (red) and Hoechst (blue). Cells were treated with LPS 1 μg·ml^{-1} with or without E5564 (1 μM) for 16 hr. Calibration bars correspond to 25 μm. (c) Microglia morphology was classified as resting (Type 1), initiating microglial activation (Type 2), activated but non-phagocytic (Type 3), and phagocytic (Type 4) according to Sanchez-Guajardo et al. (2010). Quantification of microglial phenotype subtypes (d) and cell body size (e) were evaluated in control-, OGD-, and E5564-treated organotypic slices. Data are mean ± SEM of six different experiments; *$P < .05$ compared with the untreated slices; #$P < .05$ with respect to OGD-treated slices

size of microglial cells, we observed that E5564 treatment reduced the enlargement of microglia cell bodies induced by OGD (Figure 4e). Taken together, we conclude that E5564 has a neuroprotective effect in OHCs subjected to OGD, which correlated with the percentage of microglia phenotype activation in E5564-treated OHC cultures.

3.4 | Post-stroke treatment with E5564 reduces infarct size and neuromotor outcome

Having established that E5564 has an anti-inflammatory and neuro-protective effect in different models in vitro, we next investigated

whether post-stroke pharmacological treatment with E5564 leads to an effective outcome in vivo. We used the tMCAO model of stroke in mice to evaluate the protective effects of E5564 in brain ischaemic conditions in vivo. We subjected 8- to 16-week-old male and female C57Bl/6 mice to tMCAO and treated them 1 and 4 hr post-stroke with E5564 (4 mg·kg^{-1}). Animals were treated at different time points for later assessment by staining brain sections with TTC as described in Kleinschnitz et al. (2010; Figure 5a). E5564 treatment 1 hr post-reperfusion significantly reduced infarct size (Figure 5b) in accord with previous findings in vitro. Since the stroke therapeutic window remains one of the most frequent treatment limitations due to an extremely short time frame, we extended the therapeutic onset and
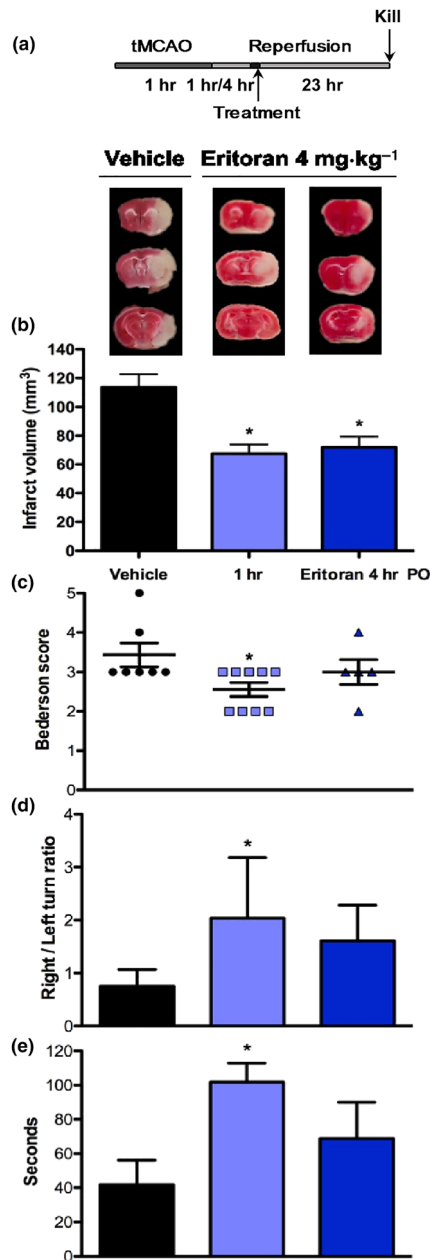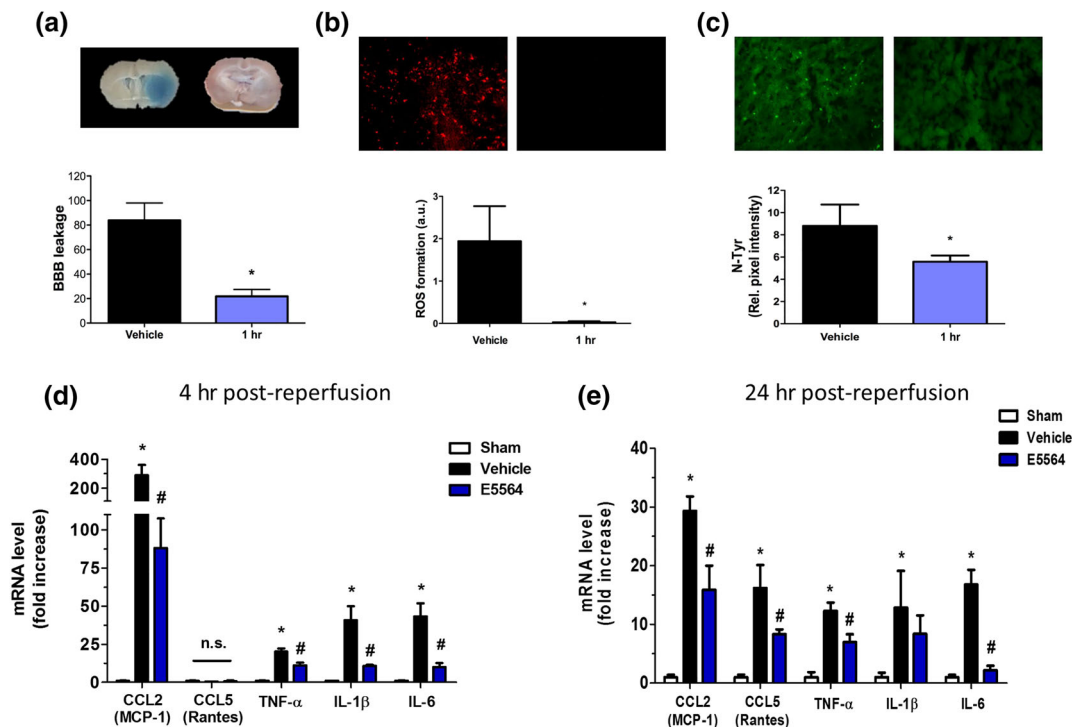
FIGURE 5 E5564 post-stroke treatment reduced infarct size and improved neuromotor functioning. (a) Adult mice were subjected to a 1 hr-transient occlusion of the middle cerebral artery (tMCAO) followed by 24 hr of reperfusion before killing. Treatment was injected i.p. 1 or 4 hr after the beginning of reperfusion; (b) 24 hr post-stroke, infarct size was reduced in mice treated with E5564 (eritoran; 4 mg·kg^{-1}), 1 hr ($*P < .05$, $n = 11$), and 4 hr post-stroke ($*P < .05$, $n = 5$) compared to non-treated (vehicle) mice. Representative pictures of the TTC stain are shown above the graphs. (b) With respect to neuromotor outcome post-treatment, the Bederson score was improved in adult mice treated with E5564 1 hr post-stroke ($*P < .05$, $n = 11$). (c) Likewise, the elevated body swing test indicated a significant increase for the right swing number/total swing number ratio in adult mice treated with E5564 1 hr post-stroke ($*P < .05$, $n = 9$). (d) Similarly, significant neuromotor improvement was detected using the four limb hanging test 1 hr after ischaemia in E5564-treated animals ($*P < .05$, $n = 11$). No neuromotor improvement was detected 4 hr post-stroke

tested E5564 4 hr post-stroke. Surprisingly, the neuroprotective effect of E5564 was preserved even with this later treatment (Figure 5b). Since neurofunctional outcome is the main clinical parameter, we additionally assessed independent neurological outcome parameters. Therefore, mice subjected to tMCAO and treated 1 and 4 hr post-stroke with E5564 were assessed using three independent neuromotor tests: Bederson score (Figure 5c), elevated body swing test (Figure 5d), and the four-limb hanging wire test (Figure 5e). All three tests were significantly improved in mice treated 1 hr post-stroke with E5564, while the animals treated 4 hr post-stroke showed no significant neuromotor improvement. Therefore, only early TLR4 inhibition 1 hr post-stroke reduced infarct volume and ameliorated neuromotor function, while the reduction in infarct volume in mice treated 4 hr post-reperfusion was not associated with any neuromotor improvement.

3.5 | E5564 prevents BBB disruption, ROS formation, and neuroinflammation post-stroke

BBB breakdown is a prominent pathology characteristic of ischaemic stroke and is associated with poor prognosis (Mao et al., 2017). Here, we first analysed how TLR4 inhibition affects the integrity of the BBB after ischaemic stroke by measuring the extravasation of Evans Blue (a vascular tracer) into the brain parenchyma. E5564 treatment 1 hr after reperfusion significantly reduced BBB disruption compared with non-treated mice (Figure 6a) suggesting that TLR4 plays a key role in microvasculature disruption post-stroke.

Ischaemia in the brain is a complex pathology involving several mechanisms, which include changes in BBB permeability evoked by increased ROS formation, and the production of cytokines and chemokines (Casas et al., 2017; Ren et al., 2018). To evaluate the role of E5564 in oxidative and nitrative stress, we assessed both ROS generation (DHE staining) and protein nitration (N-Tyr, N-tyrosine formation) in brain tissue cryosections. ROS formation and nitrosilated proteins were significantly reduced in brains treated with E5564 1 hr post-stroke compared with sham mice (Figure 6b,c). Then, we examined whether TLR4 inhibition could reduce the inflammatory response in brain ischaemia. For that, we evaluated mRNA levels of two chemokines (CCL2 and CCL5) as well as the pro-inflammatory cytokines (TNF-α, IL-1β, and IL-6) in mice treated with E5564 1 hr post-stroke. At 4 hr post-reperfusion, E5564 significantly reduced CCL2, TNF-α, IL-1β, and IL-6 levels (Figure 6e). However, at 24 hr post-reperfusion, E5564 significantly reduced mRNA levels of CCL2, CCL5 TNF-α, and IL-6, but showed no significant effect on IL-1β (Figure 6f). Therefore, E5564 significantly reduced ROS generation and inflammatory markers, which could prevent the breakdown of the BBB breakdown and would be associated with improved patient prognosis, less ischaemia-derived complications, and enhanced quality of life post-stroke.

FIGURE 6 Post-stroke treatment with E5564 prevented blood–brain barrier disruption and reduced ROS formation, protein nitrosilation, and neuroinflammation post-stroke. Adult mice were subjected to a 1 hr-transient occlusion of the middle cerebral artery (tMCAO) followed by 24 hr of reperfusion before being killed. Treatment was injected i.p. 1 hr post-reperfusion. (a) Blood–brain barrier integrity was preserved in E5564-treated animals (E5564, 4 mg·kg^{-1}) compared with non-treated (vehicle) mice 24 hr post-stroke (*$P < .05$, $n = 5$). Brain slices from a representative animal are shown above the graph. (b) E5564-treated mice showed decreased ROS formation compared to their respective non-treated animals (*$P < .05$, $n = 5$). Representative stains are shown above the graph. (c) N-Tyr positive cells were significantly reduced in treated animals while compared to non-treated mice (*$P < .05$, $n = 5$). Representative staining pictures are shown above the graph. (d–e) mRNA levels of CCL-2, CCL-5, TNF-α, IL-1β, and IL-6 were reduced in E5564-treated mice in comparison with vehicle-treated mice at 4 or 24 hr post-reperfusion respectively. Data are mean ± SEM of eight different experiments; *$P < .05$ compared with sham animals; #$P < .05$ with respect to saline-treated animals

## 3.6 | Antioxidant and anti-inflammatory effect of the TLR4 antagonist E5564 in human OCCs

Finally, we wanted to confirm the results obtained in animal models in a preliminary study in hOCCs. To study the effect of inhibiting the TLR pathway on the development of inflammatory processes in brain injuries, we investigated how E5564 could change the morphology of activated microglia in hOCCs. After 7 days in culture, hOCCs were treated with 10-μg·ml^{-1} LPS for 24 hr, to simulate the inflammatory injury induced by brain ischaemia, in the presence or absence of 1-μM E5564. LPS is a well-known TLR4 agonist that initiates a systemic inflammatory response by the innate immune system and induces an acute increase in pro-inflammatory cytokines and chemokines (Lu, Yeh, & Ohashi, 2008). hOCCs were then fixed and labelled with α-Iba1 antibody and the morphological phenotype of the microglia quantified and classified according to the different states of activation, as described above (Figure 7). E5564-dependent TLR4 inhibition reduced microglia Type 4 and increased Type 1 microglial cells in comparison with LPS alone-treated slices (Figure 7a–d). In addition, we assessed the effect of TLR4 inhibition on iNOS expression post-LPS. LPS induced an increase in iNOS expression that was attenuated after

the cotreatment with E5564 (Figure 7e). All together, these data suggest that TLR4 inhibition has a potent anti-inflammatory and neuroprotective effect in human organotypic cultures.

4 | DISCUSSION

In the present study, we provide experimental evidence that the TLR4 blocker E5564 has an anti-inflammatory and neuroprotective effect in rat, mice, and human ischaemia models both in vitro and in vivo. Blocking TLR4 reduces ROS expression and pro-inflammatory markers in LPS-stimulated and OGD-damaged microglia, actions that are involved in the neuroprotective effect of E5564 in brain ischaemia.

The crucial role of TLR4 in the pathogenesis of stroke has been demonstrated in several studies (Fang, Wang, Zhou, Wang, & Yang, 2013; Wang et al., 2013). TLR4 knockout mice have reduced brain infarct size in focal cerebral ischaemia (Kilic, Kilic, Matter, Bassetti, & Hermann, 2008). Furthermore, brain ischaemia increases TLR4 expression, leading to phosphorylation of IκB-α and translocation of NF-κB to the nucleus (Hua et al., 2007). Moreover, the TLR4 antagonist TAK-242 significantly inhibited the phosphorylation of IKKα/β and
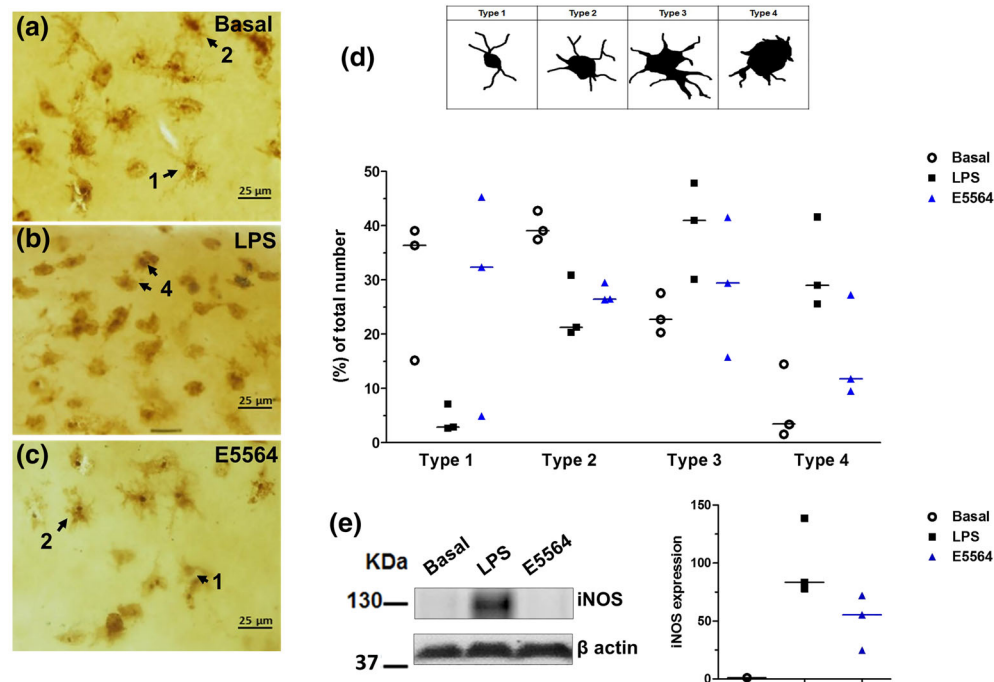
FIGURE 7 E5564 reduced microglia pro-inflammatory phenotype in human organotypic cultures. Cultures of organotypic slices were obtained using brain samples from adult patients. Slices were treated with LPS 1 μg·ml^{-1} with or without E5564 1 μM for 24 hr. After this period of time, slices were fixed and labelled with anti-*Iba1* (microglia marker). Microphotographs of control slices (a), LPS (b), and E5564 (c) are shown where black arrows indicate different examples of microglia phenotypes. (d) Quantitative analyses of different subtypes of microglia subjected to the conditions mentioned above. (e) Representative immunoblot and quantitation of iNOS expression from human brain samples treated with LPS with or without E5564. Data are scattered plot of three different cultures (a total of 600 cells per group from three different cultures associated with three different patients)

IκB-α in a mouse model of cerebral ischaemia/reperfusion (Hua et al., 2015). In fact, neurons present in infarcted brains of TLR4$^{-/-}$ mice expressed lower levels of iNOS compared to their respective wild-type littermates (Kilic et al., 2008). Here, we showed that E5564 treatment produced a significant reduction of IκB-α phosphorylation that led to reduced ROS production and iNOS overexpression presumably through the activation of NF-κB in BV2 microglial cells, mixed glia cultures, and human brain samples. It is well known that NF-κB activation leads to the induction of oxidative and nitrosative stress, so treatment with E5564 reduced ROS overproduction by presumably blocking activation of the NF-κB pathway. Nevertheless, the participation of E5564 in other routes involved in ROS/RNS production after TLR4 activation, such as TLR4-NOX4 signalling, still needs to be clarified (Suzuki et al., 2012).

Pro-inflammatory cytokines are clearly increased early after cerebral ischaemia and contribute to tissue damage. The release of pro-inflammatory markers is linked to the activation of TLR4 after acute brain injuries (Ahmad et al., 2013). Interestingly, similar time courses of TLR4 expression and TNF-α serum levels were obtained after pMCAO in rats (Tu et al., 2010). Here, we showed that by reducing IL-6, IL-1β, and TNF-α expression E5564 had an anti-inflammatory effect in vitro and in vivo, with different kinetics after reperfusion. Moreover, we also showed that E5564 prevented the increase in CCL2 and CCL5 chemokines in glia cultures post-LPS and in infarcted

mice. This mechanism might explain the effect of E5564 on BBB breakdown. Indeed, exposure to the chemokine CCL2 induces an increase in permeability in the brain endothelial monolayers through the internalization of tight junction proteins and neutralization of CCL2 (Stamatovic, Keep, Wang, Jankovic, & Andjelkovic, 2009). Therefore, the pro-inflammatory cytokine release and caspase activation subsequent to TLR4 signalling is a promising pharmacological target for ischaemic stroke therapy (Suzuki et al., 2012; Tao et al., 2015).

Microglia/macrophage are one of the most important cell types contributing to inflammatory responses. Microglia are activated after different types of neurotoxic damage. As previously mentioned, microglia can be classified under various subtypes from activated/pro-inflammatory M1 to alternatively activated/anti-inflammatory M2 (Perry, Nicoll, & Holmes, 2010). Cell branches and body size undergo huge changes under certain insults that could reflect a pro- or anti-inflammatory role (Kozlowski & Weimer, 2012). Here, we present the morphological changes in OHCs subjected to OGD and human brain microglia subjected to LPS. These data correlate with previous studies where microglia cell bodies of OHCs treated with LPS exhibited an increase in the length and area (Papageorgiou et al., 2016). Moreover, this impairment was prevented by E5564, which moved the system towards an alternatively activated/anti-inflammatory M2 phenotype. So far, our study is the first to show that the human microglia phenotype is clearly modified by blocking TLR4.

In summary, E5564 administered post-ischaemia provides a neuro-protective effect that is associated with (a) block of TLR4, (b) a reduction in ROS production and protein nitration, (c) a decrease in cytokine and chemokine release, mediated by the control of microglial pro-inflammatory phenotype, resulting in (d) an improvement in the integrity of the BBB, (e) a reduction in infarct size, and (f) the amelioration of neuromotor function.

ACKNOWLEDGEMENTS

CONFLICT OF INTEREST

The authors declare no conflicts of interest.

AUTHOR CONTRIBUTIONS

E.P. performed the majority of the in vitro experiments and those using human organotypic slices. A.I.C. performed the majority of the in vivo experiments. A.P.-A. performed some in vivo experiments and qPCR of in vivo experiments. V.G.-R. supported both in vivo and in vitro experiments. A.R.-N. and M.G.-H. performed PCR of in vitro experiments. V.F.-A. and P.N.-F. performed some in vitro experiments. J.M.R. and B.J.H.-G. provided human samples. J.M.R. helped with the study design and edited the manuscript. J.A.M., J.M., and J.E. designed the study, edited the figures, and the manuscript.

DECLARATION OF TRANSPARENCY AND SCIENTIFIC RIGOUR

This Declaration acknowledges that this paper adheres to the principles for transparent reporting and scientific rigour of preclinical research as stated in the *BJP* guidelines for Design & Analysis, Immunoblotting and Immunochemistry, and Animal Experimentation, and as recommended by funding agencies, publishers and other organisations engaged with supporting research.

ORCID

Javier Egea https://orcid.org/0000-0003-4704-3019

REFERENCES

Aertker, B. M., Bedi, S., & Cox, C. S. Jr. (2016). Strategies for CNS repair following TBI. *Experimental Neurology*, *275*(Pt 3), 411–426. https://doi.org/10.1016/j.expneurol.2015.01.008

Ahmad, A., Crupi, R., Campolo, M., Genovese, T., Esposito, E., & Cuzzocrea, S. (2013). Absence of TLR4 reduces neurovascular unit and secondary inflammatory process after traumatic brain injury in mice. *PLoS ONE*, *8*(3), e57208. https://doi.org/10.1371/journal.pone.0057208

Alexander, S. P. H., Fabbro, D., Kelly, E., Marrion, N. V., Peters, J. A., Faccenda, E., ... CGTP Collaborators (2017a). The Concise Guide to PHARMACOLOGY 2017/18: Catalytic receptors. *British Journal of Pharmacology*, *174*(S1), S225–S271. https://doi.org/10.1111/bph.13876

Alexander, S. P. H., Fabbro, D., Kelly, E., Marrion, N. V., Peters, J. A., Faccenda, E., ... CGTP Collaborators (2017b). The Concise Guide to PHARMACOLOGY 2017/18: Enzymes. *British Journal of Pharmacology*, *174*(S1), S272–S359. https://doi.org/10.1111/bph.13877

Alexander, S. P., Kelly, E., Marrion, N. V., Peters, J. A., Faccenda, E., Harding, S. D., ... CGTP Collaborators (2017). The concise guide to PHARMACOLOGY 2017/18: Overview. *British Journal of Pharmacology*, *174*(Suppl 1), S1–S16.

Arslan, F., Keogh, B., McGuirk, P., & Parker, A. E. (2010). TLR2 and TLR4 in ischemia reperfusion injury. *Mediators of Inflammation*, *2010*, 704202.

Bederson, J. B., Pitts, L. H., Germano, S. M., Nishimura, M. C., Davis, R. L., & Bartkowski, H. M. (1986). Evaluation of 2,3,5-triphenyltetrazolium chloride as a stain for detection and quantification of experimental cerebral infarction in rats. *Stroke; a Journal of Cerebral Circulation*, *17*(6), 1304–1308. https://doi.org/10.1161/01.STR.17.6.1304

Bederson, J. B., Pitts, L. H., Tsuji, M., Nishimura, M. C., Davis, R. L., & Bartkowski, H. (1986). Rat middle cerebral artery occlusion: Evaluation of the model and development of a neurologic examination. *Stroke; a Journal of Cerebral Circulation*, *17*(3), 472–476. https://doi.org/10.1161/01.STR.17.3.472

Casas, A. I., Geuss, E., Kleikers, P. W. M., Mencl, S., Herrmann, A. M., Buendia, I., ... Schmidt, H. H. H. W. (2017). NOX4-dependent neuronal autotoxicity and BBB breakdown explain the superior sensitivity of the brain to ischemic damage. *Proceedings of the National Academy of Sciences of the United States of America*, *114*(46), 12315–12320. https://doi.org/10.1073/pnas.1705034114

Chen, H., Yoshioka, H., Kim, G. S., Jung, J. E., Okami, N., Sakata, H., ... Chan, P. H. (2011). Oxidative stress in ischemic brain damage: Mechanisms of cell death and potential molecular targets for neuroprotection. *Antioxidants Redox Signal*, *14*, 1505–1517. https://doi.org/10.1089/ars.2010.3576

Curtis, M. J., Alexander, S., Cirino, G., Docherty, J. R., George, C. H., Giembycz, M. A., ... Ahluwalia, A. (2018). Experimental design and analysis and their reporting II: Updated and simplified guidance for authors and peer reviewers. *British Journal of Pharmacology*, *175*, 987–993. https://doi.org/10.1111/bph.14153

Davis, E. J., Foster, T. D., & Thomas, W. E. (1994). Cellular forms and functions of brain microglia. *Brain Research Bulletin*, *34*(1), 73–78. https://doi.org/10.1016/0361-9230(94)90189-9

Fang, H., Wang, P. F., Zhou, Y., Wang, Y. C., & Yang, Q. W. (2013). Toll-like receptor 4 signaling in intracerebral hemorrhage-induced inflammation and injury. *Journal of Neuroinflammation*, *10*, 27.

Harding, S. D., Sharman, J. L., Faccenda, E., Southan, C., Pawson, A. J., Ireland, S., ... NC-IUPHAR (2018). The IUPHAR/BPS guide to PHARMACOLOGY in 2018: Updates and expansion to encompass the new guide to IMMUNOPHARMACOLOGY. *Nucleic Acids Research*, *46*(D1), D1091–D1106. https://doi.org/10.1093/nar/gkx1121

Hu, X., Li, P., Guo, Y., Wang, H., Leak, R. K., Chen, S., ... Chen, J. (2012). Microglia/macrophage polarization dynamics reveal novel mechanism of injury expansion after focal cerebral ischemia. *Stroke; a Journal of Cerebral Circulation*, *43*(11), 3063–3070. https://doi.org/10.1161/STROKEAHA.112.659656

Hua, F., Ma, J., Ha, T., Xia, Y., Kelley, J., Williams, D. L., ... Li, C. (2007). Activation of toll-like receptor 4 signaling contributes to hippocampal neuronal death following global cerebral ischemia/reperfusion. *Journal of Neuroimmunology*, *190*(1–2), 101–111. https://doi.org/10.1016/j.jneuroim.2007.08.014

Hua, F., Tang, H., Wang, J., Prunty, M. C., Hua, X., Sayeed, I., & Stein, D. G. (2015). TAK-242, an antagonist for toll-like receptor 4, protects against acute cerebral ischemia/reperfusion injury in mice. *Journal of Cerebral Blood Flow and Metabolism: Official Journal of the International Society of Cerebral Blood Flow and Metabolism*, *35*(4), 536–542. https://doi.org/10.1038/jcbfm.2014.240

Hyakkoku, K., Hamanaka, J., Tsuruma, K., Shimazawa, M., Tanaka, H., Uematsu, S., ... Hara, H. (2010). Toll-like receptor 4 (TLR4), but not TLR3 or TLR9, knock-out mice have neuroprotective effects against focal cerebral ischemia. *Neuroscience*, *171*(1), 258–267. https://doi.org/10.1016/j.neuroscience.2010.08.054

Janssens, S., & Beyaert, R. (2003). Role of toll-like receptors in pathogen recognition. *Clinical Microbiology Reviews*, *16*(4), 637–646. https://doi.org/10.1128/CMR.16.4.637-646.2003

Kawasaki, T., & Kawai, T. (2014). Toll-like receptor signaling pathways. *Frontiers in Immunology*, *5*, 461.

Kilic, U., Kilic, E., Matter, C. M., Bassetti, C. L., & Hermann, D. M. (2008). TLR-4 deficiency protects against focal cerebral ischemia and axotomy-induced neurodegeneration. *Neurobiology of Disease*, *31*(1), 33–40. https://doi.org/10.1016/j.nbd.2008.03.002

Kilkenny, C., Browne, W., Cuthill, I. C., Emerson, M., & Altman, D. G. (2010). Animal research: Reporting *in vivo* experiments: The ARRIVE guidelines. *British Journal of Pharmacology*, *160*, 1577–1579.

Kleinschnitz, C., Grund, H., Wingler, K., Armitage, M. E., Jones, E., Mittal, M., ... Schmidt, H. H. H. W. (2010). Post-stroke inhibition of induced NADPH oxidase type 4 prevents oxidative stress and neurodegeneration. *PLoS Biology*, *8*(9), e1000479. https://doi.org/10.1371/journal.pbio.1000479

Kozlowski, C., & Weimer, R. M. (2012). An automated method to quantify microglia morphology and application to monitor activation state longitudinally in vivo. *PLoS ONE*, *7*(2), e31814. https://doi.org/10.1371/journal.pone.0031814

Lawson, L. J., Perry, V. H., Dri, P., & Gordon, S. (1990). Heterogeneity in the distribution and morphology of microglia in the normal adult mouse brain. *Neuroscience*, *39*(1), 151–170. https://doi.org/10.1016/0306-4522(90)90229-W

Liu, M., Gu, M., Xu, D., Lv, Q., Zhang, W., & Wu, Y. (2010). Protective effects of toll-like receptor 4 inhibitor eritoran on renal ischemia-reperfusion injury. *Transplantation Proceedings*, *42*(5), 1539–1544. https://doi.org/10.1016/j.transproceed.2010.03.133

Lu, Y. C., Yeh, W. C., & Ohashi, P. S. (2008). LPS/TLR signal transduction pathway. *Cytokine*, *42*(2), 145–151. https://doi.org/10.1016/j.cyto.2008.01.006

Lynn, M., Rossignol, D. P., Wheeler, J. L., Kao, R. J., Perdomo, C. A., Noveck, R., ... McMahon, F. G. (2003). Blocking of responses to endotoxin by E5564 in healthy volunteers with experimental endotoxemia. *The Journal of Infectious Diseases*, *187*(4), 631–639. https://doi.org/10.1086/367990

Mao, L., Li, P., Zhu, W., Cai, W., Liu, Z., Wang, Y., ... Hu, X. (2017). Regulatory T cells ameliorate tissue plasminogen activator-induced brain haemorrhage after stroke. *Brain: A Journal of Neurology*, *140*(7), 1914–1931. https://doi.org/10.1093/brain/awx111

McDonald, K. A., Huang, H., Tohme, S., Loughran, P., Ferrero, K., Billiar, T., & Tsung, A. (2014). Toll-like receptor 4 (TLR4) antagonist eritoran tetrasodium attenuates liver ischemia and reperfusion injury through inhibition of high-mobility group box protein B1 (HMGB1) signaling. *Molecular Medicine*, *20*, 639–648. https://doi.org/10.2119/molmed.2014.00076

Mullarkey, M., Rose, J. R., Bristol, J., Kawata, T., Kimura, A., Kobayashi, S., ... Rossignol, D. P. (2003). Inhibition of endotoxin response by e5564, a novel toll-like receptor 4-directed endotoxin antagonist. *The Journal of Pharmacology and Experimental Therapeutics*, *304*(3), 1093–1102.

Nimmerjahn, A., Kirchhoff, F., & Helmchen, F. (2005). Resting microglial cells are highly dynamic surveillants of brain parenchyma in vivo. *Science*, *308*, 1314–1318. https://doi.org/10.1126/science.1110647

Opal, S. M., Laterre, P. F., Francois, B., LaRosa, S. P., Angus, D. C., Mira, J. P., ... ACCESS Study Group (2013). Effect of eritoran, an antagonist of MD2-TLR4, on mortality in patients with severe sepsis: The ACCESS randomized trial. *Jama*, *309*(11), 1154–1162. https://doi.org/10.1001/jama.2013.2194

Papageorgiou, I. E., Lewen, A., Galow, L. V., Cesetti, T., Scheffel, J., Regen, T., ... Kann, O. (2016). TLR4-activated microglia require IFN-γ to induce severe neuronal dysfunction and death in situ. *Proceedings of the National Academy of Sciences of the United States of America*, *113*(1), 212–217. https://doi.org/10.1073/pnas.1513853113

Parada, E., Buendia, I., Navarro, E., Avendano, C., Egea, J., & Lopez, M. G. (2015). Microglial HO-1 induction by curcumin provides antioxidant, antineuroinflammatory, and glioprotective effects. *Molecular Nutrition & Food Research*, *59*(9), 1690–1700. https://doi.org/10.1002/mnfr.201500279

Parada, E., Egea, J., Buendia, I., Negredo, P., Cunha, A. C., Cardoso, S., ... López, M. G. (2013). The microglial α7-acetylcholine nicotinic receptor is a key element in promoting neuroprotection by inducing heme oxygenase-1 via nuclear factor erythroid-2-related factor 2. *Antioxidants & Redox Signaling*, *19*(11), 1135–1148.

Perry, V. H., Nicoll, J. A., & Holmes, C. (2010). Microglia in neurodegenerative disease. *Nature Reviews. Neurology*, *6*(4), 193–201.

Ren, H., Kong, Y., Liu, Z., Zang, D., Yang, X., Wood, K., ... Liu, Q. (2018). Selective NLRP3 (pyrin domain-containing protein 3) Inflammasome inhibitor reduces brain injury after intracerebral hemorrhage. *Stroke; a Journal of Cerebral Circulation*, *49*(1), 184–192. https://doi.org/10.1161/STROKEAHA.117.018904

Sanchez-Guajardo, V., Febbraro, F., Kirik, D., & Romero-Ramos, M. (2010). Microglia acquire distinct activation profiles depending on the degree of α-synuclein neuropathology in a rAAV based model of Parkinson's disease. *PLoS ONE*, *5*(1), e8784. https://doi.org/10.1371/journal.pone.0008784

Shirey, K. A., Lai, W., Scott, A. J., Lipsky, M., Mistry, P., Pletneva, L. M., ... Vogel, S. N. (2013). The TLR4 antagonist Eritoran protects mice from lethal influenza infection. *Nature*, *497*(7450), 498–502. https://doi.org/10.1038/nature12118

Stamatovic, S. M., Keep, R. F., Wang, M. M., Jankovic, I., & Andjelkovic, A. V. (2009). Caveolae-mediated internalization of occludin and claudin-5 during CCL2-induced tight junction remodeling in brain endothelial cells. *The Journal of Biological Chemistry*, *284*(28), 19053–19066. https://doi.org/10.1074/jbc.M109.000521

Stoppini, L., Buchs, P. A., & Muller, D. (1991). A simple method for organotypic cultures of nervous tissue. *Journal of Neuroscience Methods*, *37*(2), 173–182. https://doi.org/10.1016/0165-0270(91)90128-M

Suzuki, Y., Hattori, K., Hamanaka, J., Murase, T., Egashira, Y., Mishiro, K., ... Hara, H. (2012). Pharmacological inhibition of TLR4-NOX4 signal protects against neuronal death in transient focal ischemia. *Scientific Reports*, *2*, 896. https://doi.org/10.1038/srep00896

Tao, X., Sun, X., Yin, L., Han, X., Xu, L., Qi, Y., ... Peng, J. (2015). Dioscin ameliorates cerebral ischemia/reperfusion injury through the downregulation of TLR4 signaling via HMGB-1 inhibition. *Free Radical Biology & Medicine*, *84*, 103–115. https://doi.org/10.1016/j.freeradbiomed.2015.03.003

Tidswell, M., Tillis, W., Larosa, S. P., Lynn, M., Wittek, A. E., Kao, R., ... Eritoran Sepsis Study Group (2010). Phase 2 trial of eritoran tetrasodium (E5564), a toll-like receptor 4 antagonist, in patients with severe sepsis. *Critical Care Medicine*, *38*(1), 72–83. https://doi.org/10.1097/CCM.0b013e3181b07b78

Tse, M. T. (2013). Trial watch: Sepsis study failure highlights need for trial design rethink. *Nature Reviews. Drug Discovery*, *12*(5), 334. https://doi.org/10.1038/nrd4016

Tu, X. K., Yang, W. Z., Shi, S. S., Wang, C. H., Zhang, G. L., Ni, T. R., ... Song, Q. M. (2010). Spatio-temporal distribution of inflammatory reaction and expression of TLR2/4 signaling pathway in rat brain following permanent focal cerebral ischemia. *Neurochemical Research*, *35*(8), 1147–1155. https://doi.org/10.1007/s11064-010-0167-6

Vaure, C., & Liu, Y. (2014). A comparative review of toll-like receptor 4 expression and functionality in different animal species. *Frontiers in Immunology*, *5*, 316.

Wang, Y., Ge, P., & Zhu, Y. (2013). TLR2 and TLR4 in the brain injury caused by cerebral ischemia and reperfusion. *Mediators of Inflammation*, *2013*, 124614.

Yang, H., Hreggvidsdottir, H. S., Palmblad, K., Wang, H., Ochani, M., Li, J., ... Tracey, K. J. (2010). A critical cysteine is required for HMGB1 binding to toll-like receptor 4 and activation of macrophage cytokine release. *Proceedings of the National Academy of Sciences of the United States of America*, *107*(26), 11942–11947. https://doi.org/10.1073/pnas.1003893107

Yu, L., Wang, L., & Chen, S. (2010). Endogenous toll-like receptor ligands and their biological significance. *Journal of Cellular and Molecular Medicine*, *14*(11), 2592–2603. https://doi.org/10.1111/j.1582-4934.2010.01127.x